Corrosion Inhibition and Sustainable Waste Management: Evaluating the Potential of Expired Lopinavir-Ritonavir in Steel Protection

Suleiman Bulama[1*], Alhaji M. Kolo[1], Istafinus. Y. Chindo[1], Auwal. A. Mahmoud[1], Dahiru Ibrahim[2].

[1]Department of Chemistry Abubakar Tafawa Balewa University Bauchi P.M.B 0248 Bauchi State, Nigeria.

[2]Nigerian Army University Biu No. 1 Gombe Road, P.M.B 1500 Biu, Borno State Nigeria.

[*]Corresponding Author: sbulama3.sb@gmail.com

DOI: https://doi.org/10.51584/IJRIAS.2026.11030045

Received: 09 March 2026; Accepted: 17 March 2026; Published: 06 April 2026

ABSTRACT

This study investigated the potential of expired Lopinavir-Ritonavir (LPV-RTV) co-formulated antiretroviral drug, a pharmaceutical waste product, as a corrosion inhibitor for mild steel. The corrosion inhibition efficiency of expired LPV-RTV was evaluated through three complementary methods: weight loss, potentiodynamic polarization (PDP), and Scanning Electron Microscopy with Energy Dispersive X-ray Spectroscopy (SEM-EDX). The results demonstrated that expired LPV-RTV significantly enhanced the corrosion resistance of mild steel, achieving maximum inhibition efficiencies of 95.7% by weight loss and 93.0% by PDP. SEM-EDX analysis of the steel surfaces revealed the formation of a protective layer, further supporting the corrosion inhibition mechanism. These findings highlight the effectiveness of expired LPV-RTV as an efficient, eco-friendly corrosion inhibitor. The study also emphasizes the potential of utilizing expired pharmaceuticals for sustainable resource recovery, offering a viable solution for both pharmaceutical waste reduction and industrial corrosion control.

Keywords: Lopinavir-Ritonavir, PDP, Pharmaceutical waste, SEM-EDX, Weight Loss.

INTRODUCTION

Corrosion of mild steel is a major challenge in various industrial sectors, including construction, automotive, and manufacturing, where steel is commonly used in critical infrastructure. The corrosion of steel not only results in significant economic losses, but also leads to structural damage, increased maintenance costs, and environmental concerns [1, 2] To mitigate corrosion, inhibitors are often employed, especially in environments where steel is exposed to aggressive conditions, such as acidic or saline environments. While traditional corrosion inhibitors, including organic compounds, inorganic salts, and synthetic polymers, have been widely studied, many of these substances are either expensive, environmentally hazardous, or both [3]. This has led to the search for more eco-friendly**,** cost-effective**,** and sustainable alternatives for corrosion prevention.

Pharmaceutical products, especially expired drugs**,** have emerged as a promising class of green corrosion inhibitors due to their organic nature and functional groups, which can interact with metal surfaces to form protective films [4]. Among such drugs, Lopinavir (IUPAC name: [(2S,3S)-3-[(2S)-2-[(2S)-2-[(2S)-2-[(2S)-2-[(2S)-2-(3-hydroxyphenyl)thiazol-4-yl]thiazol-5-yl]thiazol-4-yl]thiazol-5-yl]thiazol-3-yl]thiazol-4-yl]thiazol-3-yl]thiazol-5-yl](2S)-2-[(2S)-2-(4-methylphenyl)-3,5-dimethyl-4H-pyrrolo[3,4-b]quinolin-1-yl]-1,4-diazepan-2-yl]thiazol-3-yl)**,** a protease inhibitor used in the treatment of HIV, is frequently co-formulated with Ritonavir **(**IUPAC name: [(2S,4S)-2-[(2S)-2-[(2S)-2-[(2S)-2-(3,4-dimethoxyphenyl)thiazol-4-yl]thiazol-5-yl]thiazol-4-yl]thiazol-5-yl]thiazol-3-yl]thiazol-4-yl](2S)-2-[(2S)-2-(3-methoxyphenyl)-4-methyl-4H-pyrrolo[3,4-b]quinolin-1-yl]-1,4-diazepan-2-yl]thiazol-3-yl**)**, another antiviral agent that acts as a pharmacokinetic enhancer [5].

The Lopinavir-Ritonavir co-formulation drug has been shown to possess corrosion inhibition properties, making it a potential candidate for controlling metal deterioration. The synergistic effect of Lopinavir and Ritonavir may

enhance the ability of this combination to prevent the corrosion of mild steel by forming a protective layer on the steel surface, thus mitigating corrosion. The pharmacokinetic enhancement offered by Ritonavir in the combination may also contribute to improving the stability and effectiveness of Lopinavir as a corrosion inhibitor.

While the corrosion inhibition properties of various expired pharmaceuticals have been explored, the specific application of the Lopinavir-Ritonavir combination for corrosion protection of mild steel remains underexplored. This study aims to investigate the corrosion inhibition efficiency of the expired Lopinavir-Ritonavir co-formulation for mild steel in acidic environment, using weight loss and potentiodynamic polarization (PDP) techniques. Scanning Electron Microscopy couple with Energy Dispersive X-ray Spectroscopy (SEM-EDX) was employed to analyze the surface morphology and elemental composition of the mild steel after exposure to the inhibitor, providing valuable insights into the corrosion inhibition mechanism.

The primary objectives of this study are to evaluate the corrosion inhibition efficiency of the Lopinavir-Ritonavir co-formulation drug on mild steel through weight loss and PDP techniques, to explore the corrosion inhibition mechanism via adsorption Isotherms and SEM-EDX analysis with a focus on surface morphology and the formation of a protective layer on the steel, and to assess the feasibility of using expired Lopinavir-Ritonavir co-formulation drug as a sustainable, eco-friendly alternative to conventional corrosion inhibitors. By addressing both the environmental issue of pharmaceutical waste and the industrial need for effective corrosion control, this study offers a novel, sustainable solution for mitigating corrosion in industrial applications.

MATERIALS AND METHODS

Materials and Test Solutions

API 5L X65 pipeline steel was used as the test material in this study. The steel was obtained from Kaduna Refining and Petrochemical Company (KRPC), Kaduna State, Nigeria. The material was originally manufactured by Vallourec Brasil and supplied to Daewoo Engineering & Construction Nigeria Ltd for maintenance and repair operations at the refinery.

The chemical composition of the steel (wt %) was: C (0.16), Mn (1.65), P (0.02), S (0.045), Si (0.50), Ni (0.50), Cr (0.05), Mo (0.50), Al (0.06), Cu (0.50), V (0.09), Nb (0.05), B (0.005), Ti (0.06), N (0.12), and Fe (97.04).

The corrosive medium was 1.0 M hydrochloric acid (HCl), prepared by appropriate dilution of analytical grade 37% HCl with distilled water. Fresh acid solutions were prepared prior to each experiment.

The expired Lopinavir-Ritonavir (200/50 mg), Mylan India. Expired 07/2023 obtain from ARD clinic of Abubakar Tafawa Balewa University Teaching Hospital Bauchi, Nigerian were used as received without further purification. The inhibitor concentrations of 50, 100, 150, 200, and 250 mg L^{-1} were prepared directly in the 1.0 M HCl solution.

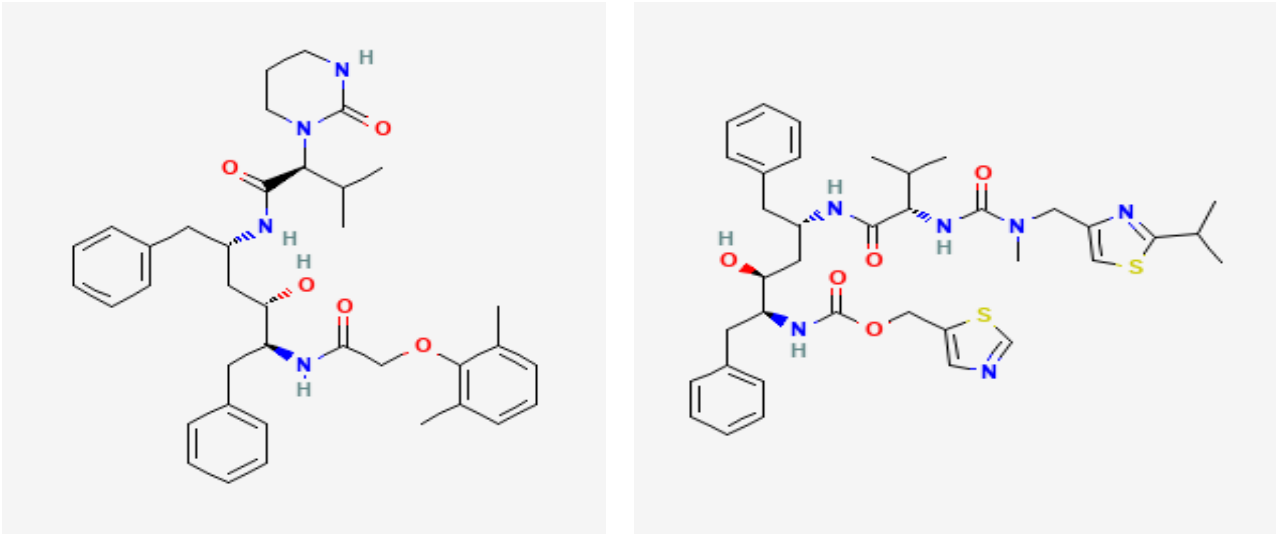

Figure. 1: Chemical Structure of Lopinavir-Ritonavir

ISSN No. 2454-6194 | DOI: 10.51584/IJRIAS |Volume XI Issue III March 2026

All experiments were conducted at temperatures of 303, 313, 323, and 333 ± 1 K using a thermostatically controlled water bath to maintain constant temperature throughout the immersion period.

Preparation of Steel Coupons

The steel coupons were prepared according to the standard cleaning procedure described in [6]. The steel Pipe was mechanically cut into rectangular specimens with dimensions of 3.0 × 1.0 × 0.1 cm.

Prior to each experiment, the coupon surfaces were sequentially polished using silicon carbide abrasive papers of grades 400, 600, 800, 1000, and 1200 grit to obtain a smooth surface finish. The polished specimens were rinsed thoroughly with distilled water, degreased with ethanol, washed with acetone, air-dried, and stored in a desiccator to prevent moisture adsorption before use.

Preparation of LPV-RTV solution

Four tablets of Lopinavir-Ritonavir (LPV-RTV), each containing 200 mg of Lopinavir and 50 mg of Ritonavir, were carefully crushed into a fine powder using a mortar and pestle. The following steps were then performed to prepare the solution [7]:

Crushing and Dissolving the Tablets;

The crushed powder was gradually mixed with a small volume of distilled water to form a smooth paste. Additional distilled water was then added in small increments to facilitate complete dissolution. The mixture was stirred thoroughly to ensure that the drugs were uniformly dispersed.

Preparing the Final Solution

The prepared paste was transferred to a 100 mL glass bottle, and the final volume was adjusted to 100 mL by adding more distilled water. The solution was shaken vigorously to ensure complete dissolution of the active pharmaceutical ingredients (APIs), Lopinavir and Ritonavir.

Concentration and Dosage

The resulting solution was designed so that each 5 mL of the prepared syrup contained the equivalent of 50 mg of the combined drug, i.e., 40 mg of Lopinavir and 10 mg of Ritonavir.

Preparation of the Stock Solution for Corrosion Studies

From the prepared syrup, 5 mL, 10 mL, 15 mL, 20 mL, and 25 mL aliquots were measured and transferred into separate 1000 mL volumetric flasks. Each flask was filled with approximately 500 mL of 1.0 M hydrochloric acid (HCl) solution. The mixtures were then shaken vigorously to ensure uniform distribution of the drugs in the acidic medium.

Final Volume Adjustment

After shaking, additional 1.0 M HCl solution was added to each flask until the total volume reached the 1000 mL mark, ensuring that the final concentration of the Lopinavir-Ritonavir co-formulation was adequately diluted for corrosion inhibition studies.

Weight Loss Measurements

Gravimetric (weight loss) measurements were performed according to the immersion test method described in [8]. Each pre-weighed steel coupon was immersed in 200 mL of 1.0 M HCl solution in the absence (blank) and presence of different concentrations of LPV-RTV (50–250 mg L^{-1}).

The immersion period was fixed at 3 hours interval at 303, 313, 323, and 333 ± 1 K. After immersion, the specimens were removed and cleaned to eliminate corrosion products following [6] procedures. The cleaning

ISSN No. 2454-6194 | DOI: 10.51584/IJRIAS |Volume XI Issue III March 2026

process involved immersion in 20% NaOH solution containing 100 g L^{-1} zinc dust for 2–5 minutes. The specimens were then scrubbed gently under running tap water using a soft bristle brush, rinsed thoroughly, degreased with ethanol, washed with acetone, dried, and reweighed.

All measurements were performed in triplicate to ensure reproducibility, and the average weight loss values were recorded. The corrosion rate (CR), inhibition efficiency (%IE), and surface coverage (θ) were calculated using standard gravimetric equations [9].

To determine the weight loss due to corrosion, the initial and final weights of the mild steel specimen are measured. The weight loss (w) in milligrams is calculated by subtracting the final weight from the initial weight of the specimen. The equation for weight loss is as follows:

$$W_i - W_f = w \quad (1)$$

Where; w is total weight loss, W_i and W_f are the initial weight before immersion and after respectively.

Corrosion Rate (CR)

In order to quantify the corrosion rate of mild steel in the absence and presence of the corrosion inhibitor, we use the formula, which relates the corrosion rate to the total weight loss and period of immersion:

$$\text{Corrosion rate(mmpy)} = \frac{87.6w}{DAT} \quad (2)$$

Where w = Total weight loss (mg), D = density of specimen (g/cm^3), A = Area of specimen (square meter) and T= period of immersion (hour) and 87.6 is a conversion factor. The density of the API 5L X65 is 7.85 g/cm^3.

Surface Coverage (θ)

To determine the effectiveness of the corrosion inhibitor, the surface coverage (θ) is calculated using the ratio of the weight loss of mild steel in the presence and absence of the inhibitor and subtract from one. The surface coverage represents the fraction of the metal surface that is covered by the inhibitor molecules, which prevents the electrochemical reactions responsible for corrosion. The formula for calculating surface coverage is given by:

$$\theta = \left(1 - \frac{w_1}{w_2}\right) \quad (3)$$

Where; $w_1$and $w_2$are the weight losses (g) for metal in the presence and absence of inhibitor respectively.

Inhibition Efficiency (%IE)

The inhibition efficiency (%IE) quantifies the extent to which the corrosion rate is reduced by the presence of an inhibitor. It is calculated by multiplying the value of surface coverage by 100. A higher value of %IE indicates a more effective inhibitor. The formula for inhibition efficiency is given by:

$$\%IE = \left(1 - \frac{w_1}{w_2}\right) \times 100 \quad (4)$$

SEM-EDX Analysis

The surface morphology of the API 5L X65 steel coupons, following immersion in a 1.0 M HCl solution for 3 hours at 303 K in the presence and absence of inhibitors, was analyzed using a Phenom ProX SEM-EDX (Netherlands).

Potentiodynamic Polarization Studies

Surface preparation of the working electrode (WE)

Standard procedure described in [10, 6] were adopted for the preparation of the working electrode and measurement. The preparation was performed with sequential wet grind with 400, 600, 800 and 1000 grit SiC

ISSN No. 2454-6194 | DOI: 10.51584/IJRIAS |Volume XI Issue III March 2026

until previous coarse scratches were removed and smooth polished surface was achieved. Then washed with distilled water, degreased with ethanol and raised with acetone and air dried.

Potentiodynamic Polarization (PDP) Measurement Procedure

The working electrode (API 5L X65) with an exposed surface area of 1 cm^2**,** the reference electrode (saturated calomel electrode, SCE), and the counter electrode (platinum, Pt) were assembled into a three-electrode electrochemical cell. 100 mL of the test solution was transferred into the polarization cell, which was then connected to a potentiostat or electrochemical workstation**.**

The system was allowed to establish the open circuit potential (OCP) of the working electrode, ensuring a stable reading before proceeding with polarization measurements.

Potentiodynamic polarization measurements were carried out by scanning the potential of the working electrode (WE**)** from -0.1 V to +0.1 V relative to the reference electrode (SCE) at a scan rate of 1 mV/sec**.** The potential was scanned in both anodic and cathodic directions to obtain the complete polarization curve.

The test was repeated for each concentration of the inhibitor solution to evaluate the impact of varying inhibitor concentrations on the corrosion behavior of the mild steel.

From the resulting polarization curves, the corrosion current density (i_{corr}) and corrosion potentials (E_{corr}) was determined using Tafel extrapolation (via the linear portions of the anodic and cathodic branches of the polarization curve).

The inhibition efficiency (%IE) of the inhibitor was calculated using the following formula:

$$\%IE = \frac{i^{o}_{corr} - i_{corr}}{i^{o}_{corr}} \times 100 \quad (5)$$

Where i^{o}_{corr} and i_{corr} are the corrosion current densities in the absence and presence of the inhibitor.

RESULTS AND DISCUSSIONS

The results obtained from the weight loss measurements, including corrosion rate (CR), surface coverage (θ), and inhibition efficiency (%IE), are presented in Table 1.

Table. 1. Shows the Corrosion parameters of API 5L X 65 mild steel from weight loss measurement.

Inh.	Surface Coverage				Corrosion Rate (mm/yr)				Inhibition efficiency			
(mg/l)	303K	313K	323K	333K	303 K	313 K	323 K	333 K	303 K	313K	323K	333K
Blank	-	-	-	-	0.0101	0.0154	0.0238	0.0376	-	-	-	-
50	0.652	0.579	0.559	0.366	0.0032	0.0065	0.0117	0.0238	65.2	57.9	55.9	36.6
100	0.652	0.632	0.576	0.409	0.0032	0.0057	0.0101	0.0222	65.2	63.2	57.6	40.9
150	0.739	0.684	0.610	0.430	0.0024	0.0048	0.0093	0.0214	73.9	68.4	61.0	43.0
200	0.870	0.737	0.644	0.452	0.0012	0.0040	0.0085	0.0206	87.0	73.7	64.4	45.2
250	0.957	0.763	0.695	0.527	0.0004	0.0036	0.0073	0.0178	95.7	76.3	69.5	52.7

The data clearly show that inhibition efficiency increases as the concentration of the inhibitor rises. This observation implies that, at higher concentrations, more inhibitor molecules are able to adsorb onto the surface of mild steel, effectively enhancing the coverage of the surface and blocking the active corrosion sites. Consequently, this results in a significant reduction in the metal's dissolution rate in the aggressive medium.

This trend aligns with the adsorption-controlled corrosion inhibition mechanisms that have been widely discussed in the literature [11]. As the inhibitor concentration increases, more adsorption sites on the metal surface are occupied by the inhibitor molecules, leading to the formation of a protective film. The increase in inhibition efficiency thus correlates with a notable decrease in corrosion rate, which further supports the protective nature of the inhibitor [12; 13].

ISSN No. 2454-6194 | DOI: 10.51584/IJRIAS |Volume XI Issue III March 2026

At the optimum inhibitor concentration studied, the highest recorded inhibition efficiency was 95.7%, indicating a strong corrosion protection effect. This high efficiency reflects the significant interaction between the inhibitor molecules and the steel surface, resulting in the formation of a dense, adherent protective film that effectively shields the metal from the corrosive medium.

Temperature Dependence and Thermodynamic Parameters

The effect of temperature on the inhibition process revealed that an increase in temperature results in a decrease in inhibition efficiency. This inverse relationship is typically attributed to several factors: (i) acceleration of the metal dissolution process due to increased kinetic energy of the reacting species, (ii) an increase in desorption rate of inhibitor molecules from the metal surface, and (iii) the alteration of adsorption mechanisms due to unfavorable thermodynamic conditions at higher temperatures [14; 15]. The reduced inhibition efficiency at elevated temperatures indicates that the adsorption of the inhibitor may involve predominantly physical adsorption**,** which is less stable at higher temperatures compared to chemical adsorption [16].

Thermodynamic parameters such as activation energy (E_a)**,** adsorption free energy ($\Delta G°_{ads}$)**,** enthalpy ($\Delta H°$)**,** and entropy ($\Delta S°$)**** play a crucial role in understanding the interaction between the inhibitor molecules and the metal surface. These parameters can be derived from the temperature dependence of the corrosion rate and inhibition efficiency.

Adsorption Isotherms

Two widely used adsorption models, the Langmuir and Temkin isotherms, were applied to analyze the adsorption behavior of the LPV-RTV onto the steel surface. Results indicated that the adsorption is consistent to Langmuir isotherm.

Langmuir adsorption isotherm is described by the following equation;

$$\log\frac{C}{\theta} = -\log K_{ads} + \log C \qquad (6)$$

A plot of $\log\frac{C}{\theta}$ verse log C from equation 9, a straight line was obtain with an intercept equal $-\log K_{ads}$ as shows in Fig 2.

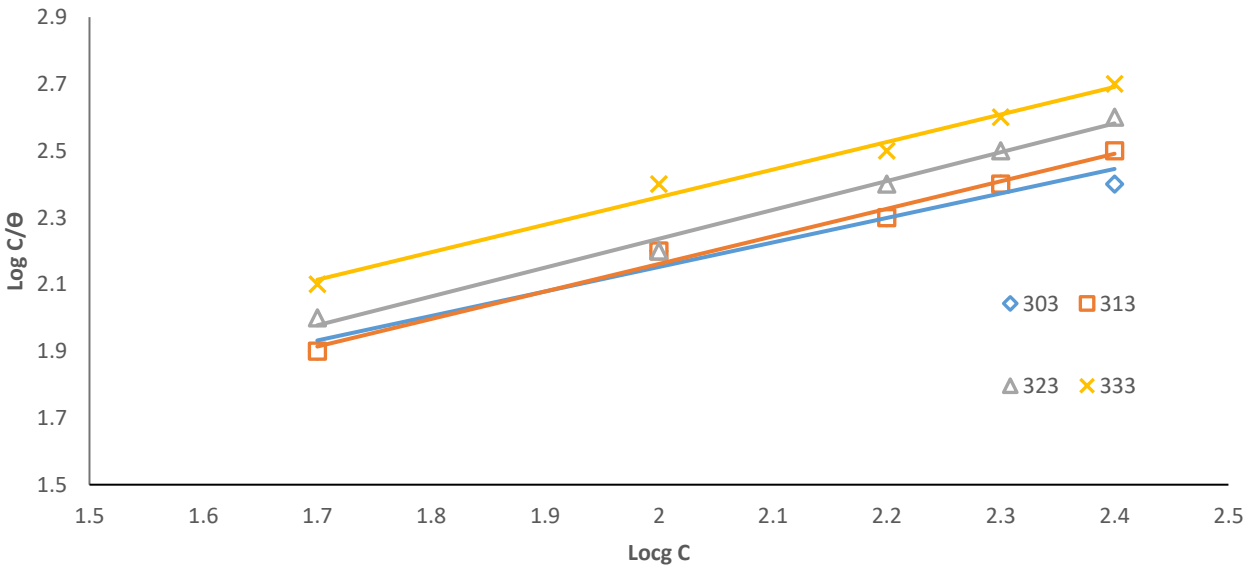

Figure. 2*:* Langmuir adsorption isotherm for LPV-RTV

ISSN No. 2454-6194 | DOI: 10.51584/IJRIAS |Volume XI Issue III March 2026

Adsorption Free Energy ($\Delta G°_{ads}$)

The adsorption free energy ($\Delta G°_{ads}$) is an important thermodynamic parameter that provides information about the spontaneity of the adsorption process and is related with equilibrium constant of adsorption K_{ads} in the following equation:

$$\Delta G^{o}_{ads} = -2.303RT\log(55.5K_{ads}) \quad (7)$$

Where ΔG^{o}_{ads}= Gibbs free energy, R= Molar gas constant, T= absolute temperature and K_{ads} = the equilibrium constant for adsorption.

The values of ΔG^{o}_{ads} calculated were listed together with the adsorption parameters evaluated from Fig, 3 in Table 2 below.

Table. 2: Isotherm parameters for the Adsorption of inhibitor on to the surface of API 5l X65 steel in 1.0 M HCl at various Temperatures.

Adsorption Isotherm	Inhibitor	Temp (K)	Slope	Intercept	$\mathbf{K_{ads}}$	$\Delta \boldsymbol{G_{ads}}$ (kJmol^{-1})	R^2
Langmuir	LPV-RTV	303	0.7338	0.6844	4.84	-14.09	0.9641
		313	0.8247	0.5117	3.25	-13.50	0.9881
		323	0.8636	0.5091	3.23	-13.94	0.9902
		333	0.8247	0.7117	5.15	-15.66	0.9881

A negative value of ΔG^{o}_{ads} suggests that the adsorption of the inhibitor on the metal surface is spontaneous, while a highly negative ΔG^{o}_{ads}implies a strong interaction between the inhibitor and the metal surface. A value of ΔG^{o}_{ads}more negative than -40 kJ/mol typically indicates physisorption**,** whereas values more negative than -80 kJ/mol are associated with chemisorption [17].

The calculated value of ΔG^{o}_{ads} turns out to be negative indicating that the adsorption of Lopinavir-Ritonavir is spontaneous and proceed via physical adsorption with the value which range between (-14 to -16 kJmol^{-1}) which were less the physisorption threshold value of -40 kJmol^{-1} .

Activation Energy (E_a)

The activation energy (E_a) provides insight into the energy required to initiate the corrosion process. A higher activation energy typically suggests that the corrosion process is more difficult to initiate, which indicates stronger inhibition [18]. The activation energy can be calculated using the Arrhenius equation:

$$\log CR = -\frac{E_a}{2.303RT} + \log A \quad (8)$$

Where CR is corrosion rate, R the molar gas constant (8.314 J/mol/K), T is the absolute temperature and A is the Arrhenius constant respectively.

Plotting natural logarithm of the corrosion rate (log CR) verse 1/T in absence and presence of the inhibitor at various concentrations the E_a values were evaluated from their slope and listed in Table 2, with other thermodynamic parameters (Fig. 3).

ISSN No. 2454-6194 | DOI: 10.51584/IJRIAS |Volume XI Issue III March 2026

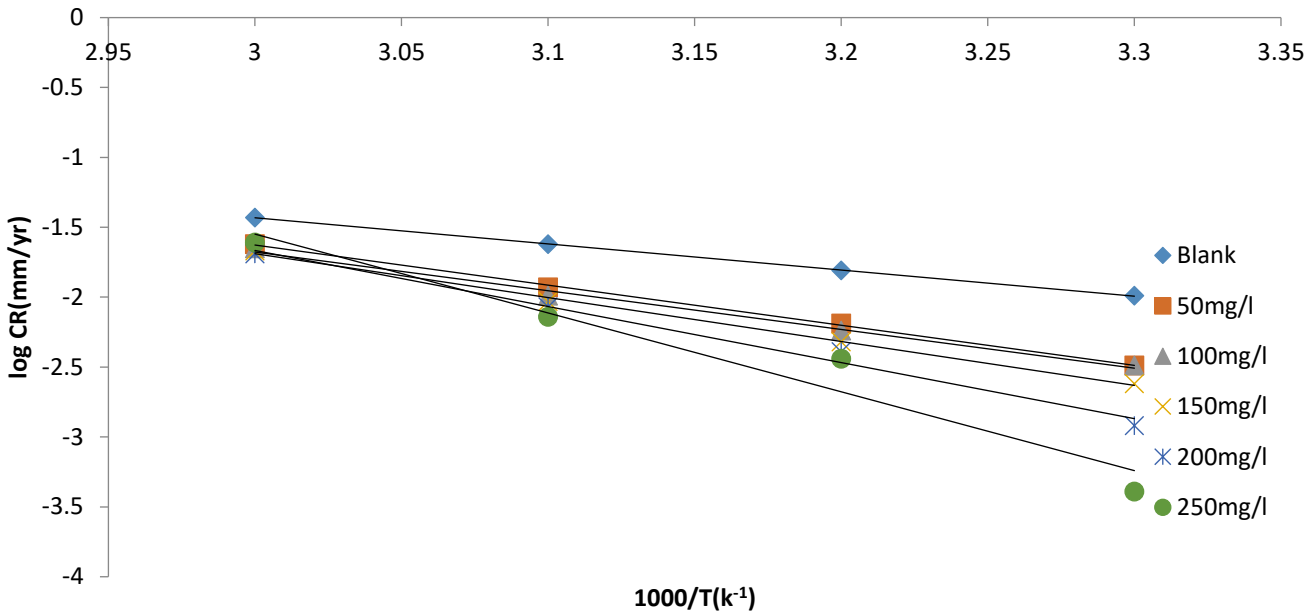

Figure. 3: Arrhenius plot for LPV-RTV

Enthalpy (ΔH*) and Entropy (ΔS*)

The Van't Hoff equation is used to relate the temperature dependence of the rate constant (or corrosion rate). By examining the temperature dependence, we can extract the activation parameters such as the enthalpy and entropy of activation. The equation is given by;

$$\log\frac{CR}{T} = \left[\log\left(\frac{R}{Nh}\right) + \frac{\Delta S^*}{2.303R}\right] - \frac{\Delta H^*}{2.303RT} \qquad (9)$$

Where h is the plank's constant and N is the Avogadro's number, respectively.

A plot of $\log\frac{CR}{T}$ verse $\frac{1}{T}$ gave a straight line with a slope of $\frac{-\Delta H^*}{2.303R}$ and intercept of $[\log\left(\frac{R}{Nh}\right) + \frac{\Delta S^*}{2.303R}]$, from which the activation thermodynamics parameters (ΔH^*) and (ΔS^*) were evaluated from Fig. 4, and summarize in Table 3.

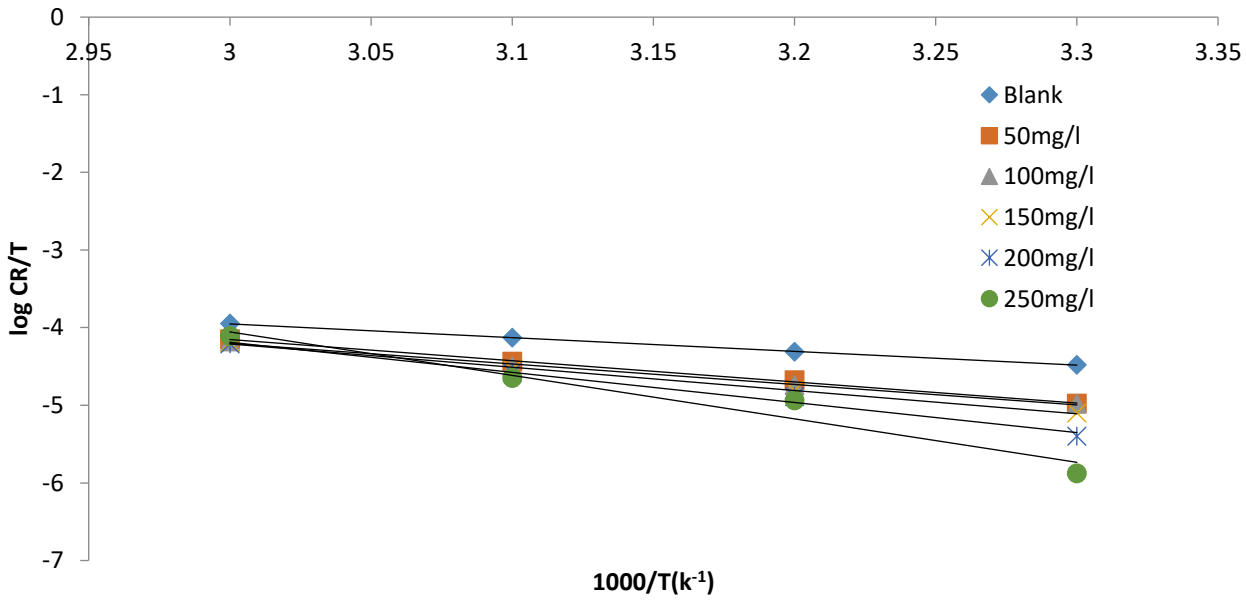

Figure. 4*:* Transition state plot for LPV-RTV.

ISSN No. 2454-6194 | DOI: 10.51584/IJRIAS |Volume XI Issue III March 2026

Table. 3: Thermodynamic parameters for corrosion inhibition of API 5L X65 mild steel in absence and present of an inhibitor.

Inhibitor Conc.(mg/L)	Ea (kJ/mol)	$-\Delta H^*$ (kJ/mol)	$-\Delta S^*$ (kJ/mol)
Blank	35.81	33.90	223.63
50	54.96	52.28	274.94
100	53.05	56.30	282.19
150	60.13	57.45	289.36
200	76.79	74.30	340.33
250	108.01	107.24	441.69

The negative values of enthalpy (ΔH***)** indicate that the adsorption of the inhibitor onto the steel surface is exothermic, meaning that the process releases heat, and the interaction between the inhibitor molecules and the metal is thermodynamically favorable [19, 20]. A more negative ΔH* value suggests a stronger interaction between the inhibitor and the steel surface, which is consistent with stronger chemisorption or physisorption mechanisms, depending on the inhibitor type [16]. It was observed that as the inhibitor concentration increased, the ΔH* value became more negative, suggesting that a higher concentration of inhibitor molecules adsorbed onto the steel surface. This leads to the formation of a stronger protective film on the surface, effectively shielding the steel from the corrosive medium [21].

The entropy (ΔS*) of adsorption is another important thermodynamic parameter in corrosion studies, as it complements the information provided by enthalpy (ΔH*). ΔS* influences the surface coverage and the molecular arrangement of the inhibitor on the metal surface. Positive values of ΔS* indicate a more disordered arrangement of inhibitor molecules, which can reduce surface coverage and, consequently, lower the inhibition efficiency [22]. On the other hand, negative ΔS* values suggest that the formation of activated complexes during the adsorption process involves an association step rather than dissociation, indicating a decrease in disorder as the inhibitor molecules organize on the metal surface [23]. This behavior is commonly observed when the inhibitor molecules adopt a more ordered structure upon adsorption, which strengthens the protective film and improves corrosion resistance.

The ΔS* values recorded in Table 3, show a decreasing trend with increasing inhibitor concentration, indicating that more inhibitor molecules were adsorbed onto the steel surface. As the concentration of the inhibitor increased, the molecules became more densely packed, reducing the disorder in the system. This aggregation of inhibitor molecules enhances the surface coverage, leading to increased inhibition efficiency and a significant reduction in corrosion rates. Thus, the thermodynamic data support the idea that higher concentrations of inhibitors form a more stable and ordered protective layer on the steel surface, contributing to better corrosion protection.

Potentiodynamic Polarization (PDP)

The Potentiodynamic Polarization (PDP) results for mild steel in the presence of the Lopinavir-Ritonavir (LPV-RTV) co-formulation drug clearly demonstrate the corrosion inhibition efficiency of the compounds. As expected, inhibition efficiency increased with the concentration of the LPV-RTV inhibitor. The polarization curves (Fig. 5) reveal that with rising inhibitor concentrations, the corrosion current density (i_{corr}) significantly decreased, while the corrosion potential (E_{corr}) shifted towards more positive values, indicating a protective effect of the inhibitor. Table 4 summarized the PDP parameters along with the corrosion rate and inhibition efficiencies at various concentration.

Table: 4**:** Potentiodynamic Polarization Parameter and Inhibition Efficiencies for the Corrosion inhibition of API 5L X65 steel in 1 M HCl

Inhibitor	Conc mg/L	$-E_{corr}$ mV/SCE	i_{corr} mA cm^{-2}	β_a mV dec^{-1}	β_c mV dec^{-1}	θ	%IE	CR (mpy)
LPV-RTV	Blank	489	3.070	132.4	141.5	-	-	1.404E3
	50	606	0.446	153.5	129.5	0.855	85.5	203.9

ISSN No. 2454-6194 | DOI: 10.51584/IJRIAS |Volume XI Issue III March 2026

	100	700	0.416	142.2	121.7	0.864	86.4	190.1
	150	663	0.401	153.1	126.0	0.870	87.0	183.3
	200	601	0.330	130.7	118.8	0.893	89.3	165.1
	250	594	0.230	146.1	1319	0.930	93.0	150.6

At the optimal inhibitor concentration, the highest recorded inhibition efficiency was 93.0%. This was accompanied by a significant shift in the corrosion potential (E_{corr}) from -489 mV/SCE for the blank to -594 mV/SCE in the presence of the inhibitor. The observed positive shift of +105 mV/SCE suggests that LPV-RTV molecules are adsorbing onto the mild steel surface, forming a protective film that effectively hinders electrochemical reactions, thus mitigating corrosion. In addition, the corrosion current density (i_{corr}) decreased substantially from the blank solution, indicating that LPV-RTV inhibits the electrochemical reactions responsible for corrosion.

In accordance with standard inhibitor classification, a shift in E_{corr} greater than ±85 mV/SCE generally indicates that the inhibitor predominantly influences either the anodic or cathodic reaction [24, 25]. The observed shift of +105 mV/SCE, exceeding this threshold, is consistent with the behavior of an anodic inhibitor. Specifically, the positive shift in E_{corr} suggests that LPV-RTV primarily affects the anodic reaction, which involves metal dissolution. This is characteristic of anodic inhibitors, which reduce metal dissolution rates without significantly impacting the cathodic reaction [26, 27].

These findings support an adsorption controlled corrosion inhibition mechanism, where the inhibitor molecules occupy active sites on the steel surface, thereby inhibiting electrochemical reactions at the anodic sites [28]. The polar functional groups of LPV and RTV likely facilitate the formation of a protective layer, thereby reducing the metal's reactivity with the corrosive medium.

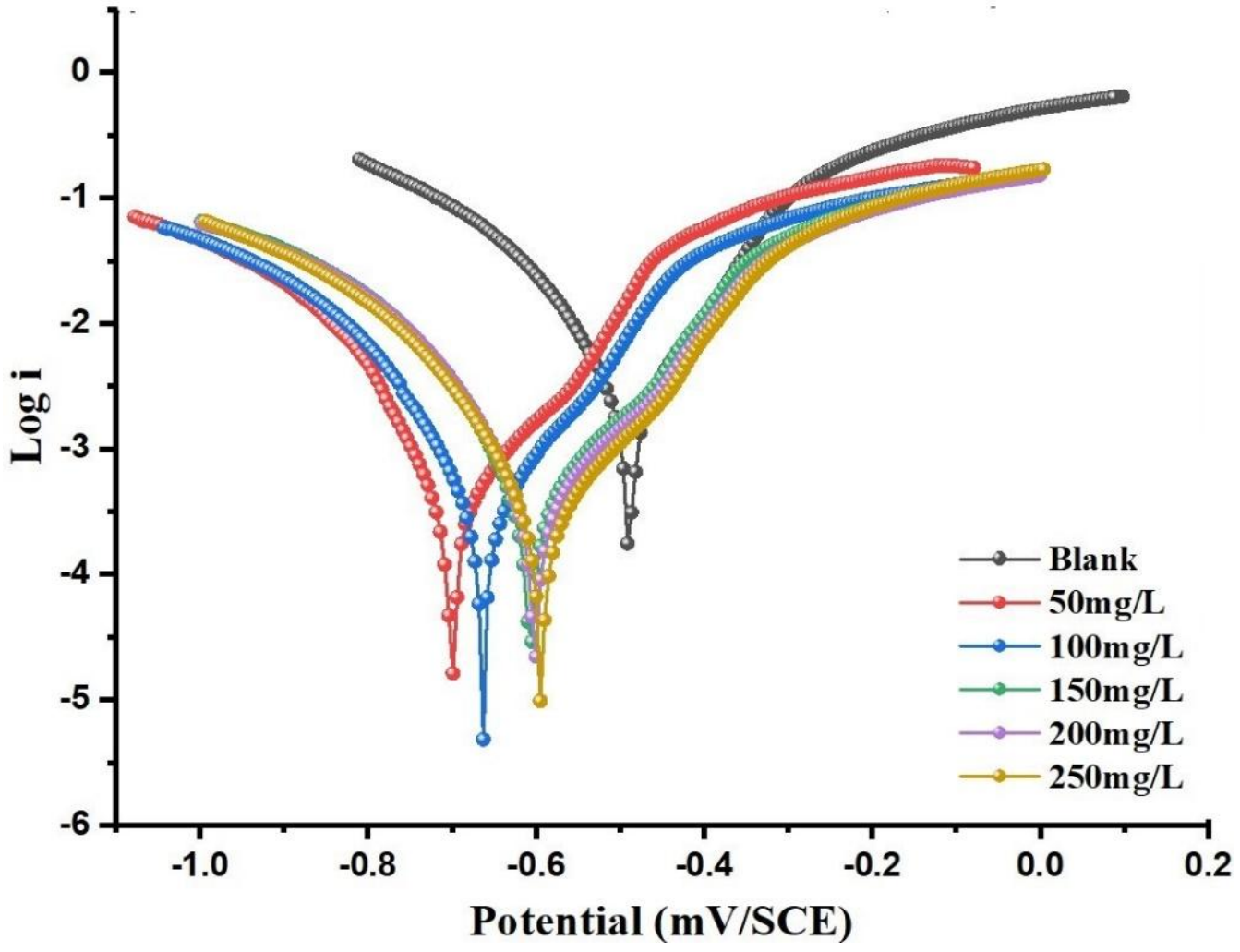

Figure 5: Tafel plot for the inhibition of API 5L X65 steel by LPV/RTV.

ISSN No. 2454-6194 | DOI: 10.51584/IJRIAS |Volume XI Issue III March 2026

The Tafel slopes for both the anodic and cathodic reactions remained relatively constant, confirming that the LPV-RTV inhibitor mainly affects the corrosion current density, without altering the fundamental reaction mechanisms of the metal [29, 30].

SEM and EDX Analysis

The surface morphology of the steel before and after exposure to the corrosive medium, as well as after the application of the inhibitor, was examined using Scanning Electron Microscopy (SEM) as show in Fig. 6.

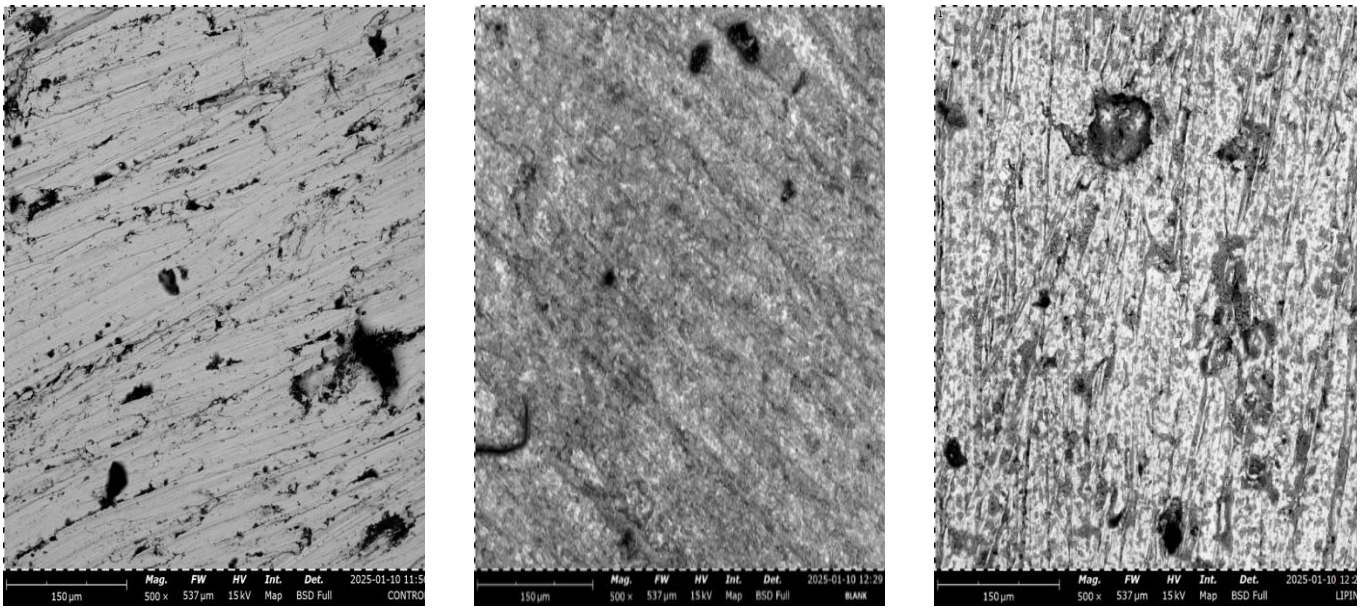

a) SEM image of untreated API 5L X65 polished coupon

b) SEM image in the absence of inhibitor (treated with HCl)

c) SEM image in the presence of inhibitor.

Figure. 6*:* Surface morphology of API 5L X65 in the absence and presence of inhibitor.

SEM images of the steel surface in its pristine state (a) reveal a smooth, clean surface, typical of untreated metal. However, after exposure to the corrosive medium, the surface becomes significantly pitted (b), indicating active corrosion, with the formation of corrosion products and surface degradation due to the interaction between the metal and the corrosive solution.

The pitting and rough surface morphology are indicative of general corrosion, which leads to the deterioration of the steel surface [31].

In contrast, the steel surface exposed to the corrosive medium in the presence of the inhibitor shows a much smoother surface (c)**,** with minimal signs of corrosion or pitting. This suggests that the inhibitor effectively reduced metal dissolution and protected the surface. The smoothness and uniformity of the surface indicate that the inhibitor forms a protective film, which acts as a barrier, preventing the corrosive agents from interacting with the metal [29]. The SEM images strongly suggest that the inhibitor has a significant role in mitigating corrosion damage and stabilizing the API steel surface.

EDX Analysis

To further support the SEM findings, Energy Dispersive X-ray (EDX) spectroscopy was used to analyze the elemental composition of the steel surface before and after exposure to the corrosive solution and inhibitor. The EDX spectra of the untreated steel show (Fig. 7) a high intensity of iron (Fe) peaks, indicating that the surface is predominantly composed of the steel substrate. After exposure to the corrosive medium, the EDX spectrum shows (Fig. 8) additional peaks for oxygen (O) and chlorine (Cl**)**, confirming the formation of corrosion products such as iron oxides and chloride salts, which are commonly formed in acidic environments [32, 33].

ISSN No. 2454-6194 | DOI: 10.51584/IJRIAS |Volume XI Issue III March 2026

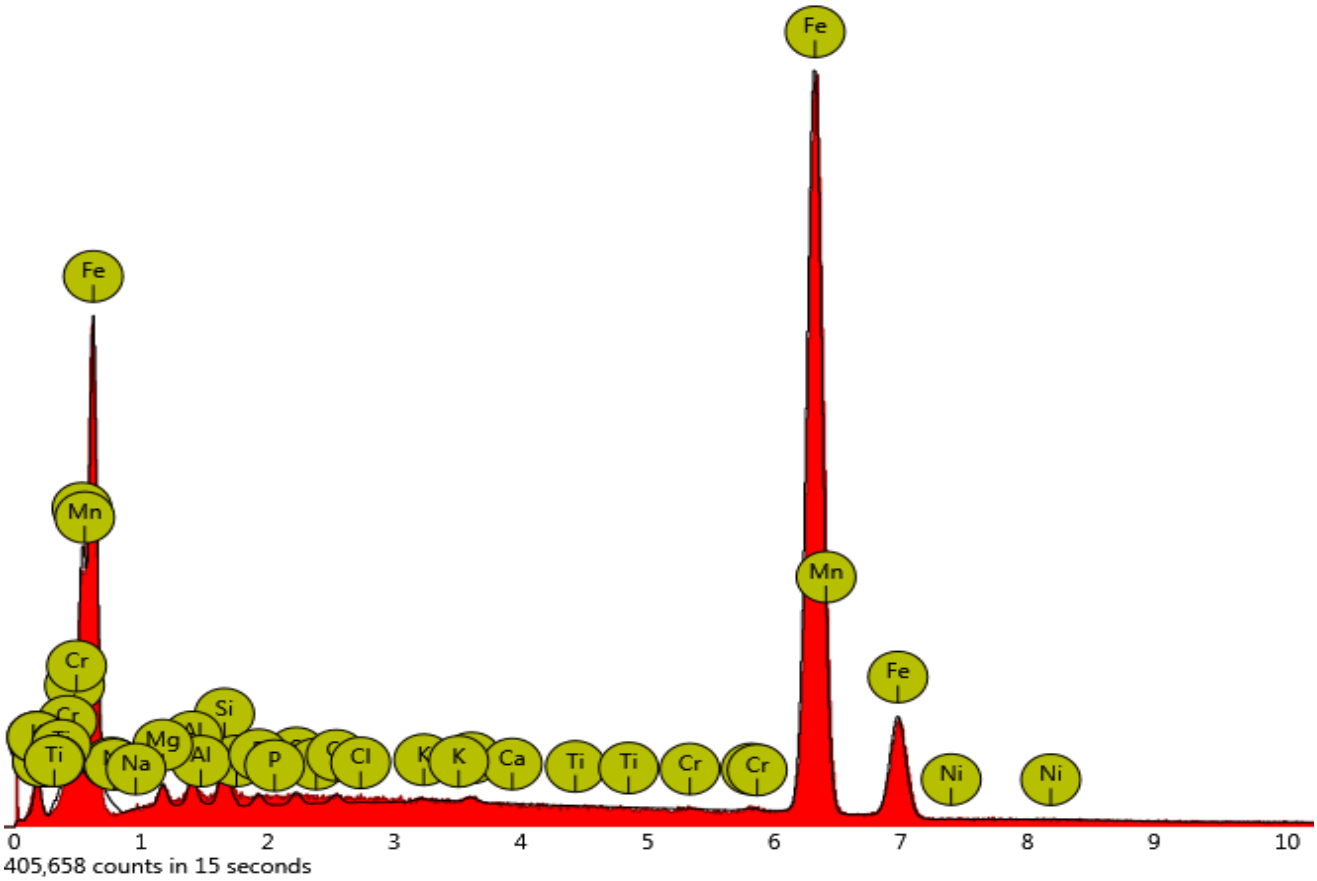

Figure. 7: EDX spectrum of untreated (Blank) API 5L X65 steel

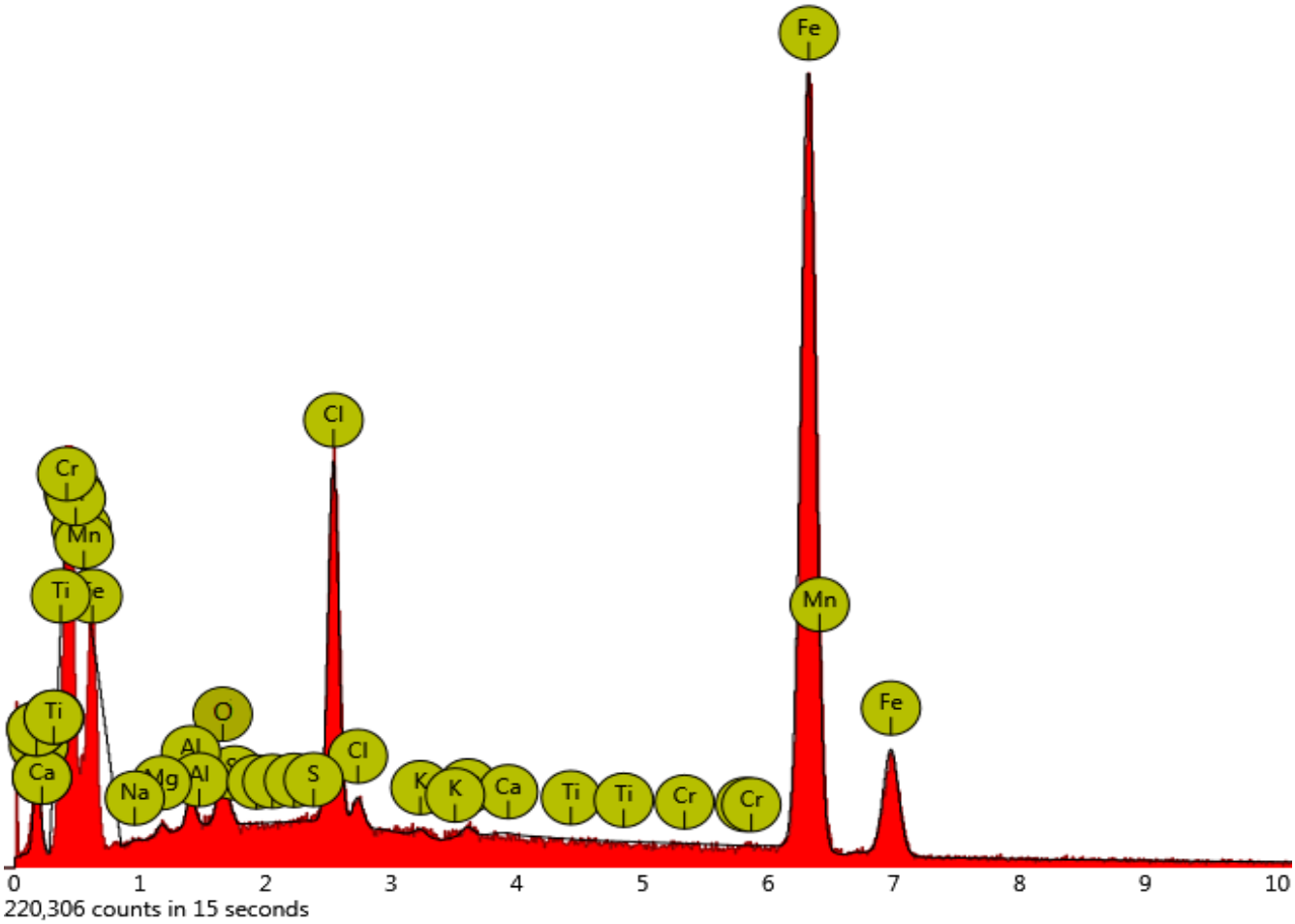

Figure.8: EDX spectrum of treated API 5L X65 steel in the presence acid.

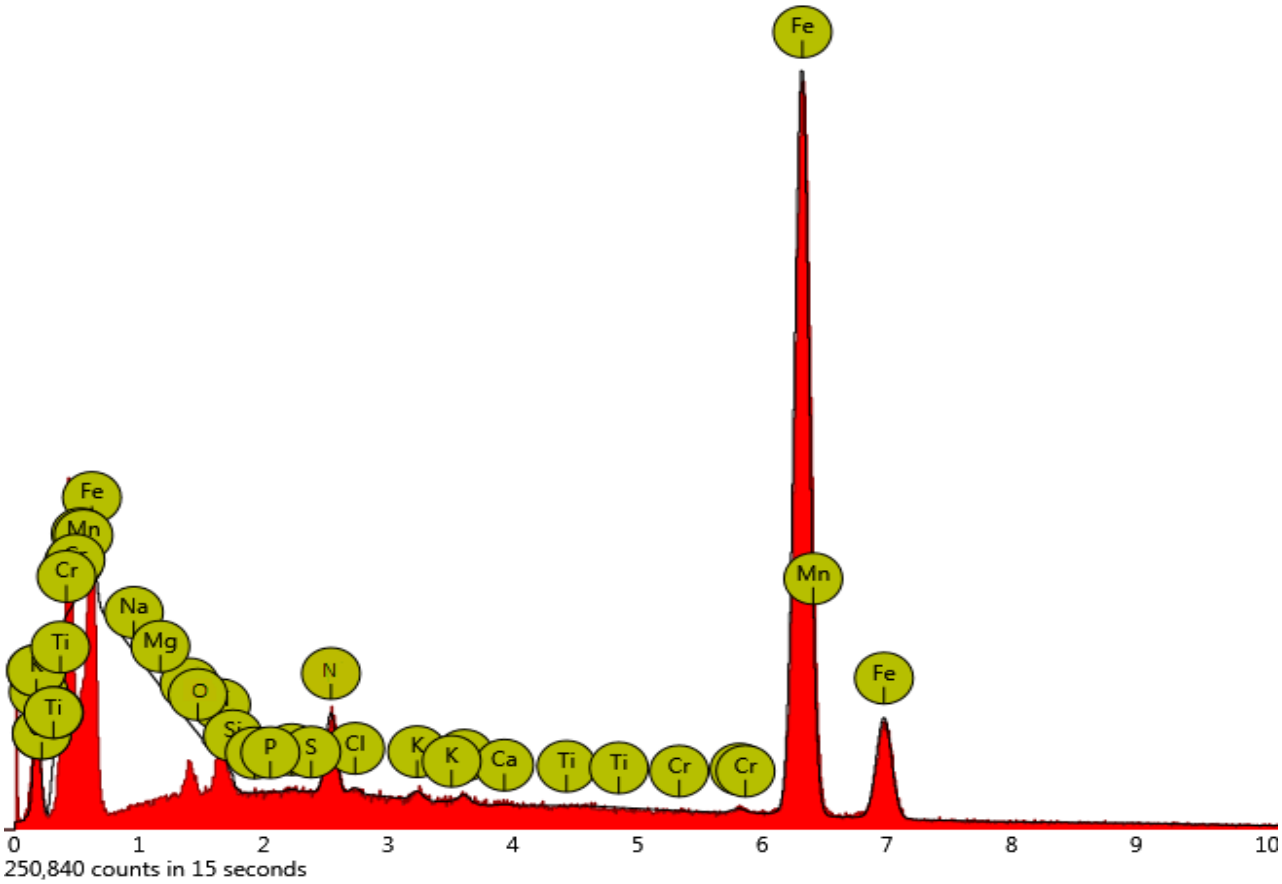

Figure. 9: EDX spectrum of treated API 5L X65 steel in the presence of LPV-RTV drug.

Upon exposure to the expired LPV-RTV as corrosion inhibitor, the EDX spectra (Fig. 9) reveal a decrease in the intensity of the chlorine (Cl) peak and the appearance of nitrogen (N), Sulphur (S), and oxygen (O) peaks. The appearance of these peaks (N, S & O) confirms the adsorption of the drug molecules and the formation of a protective film on the steel surface, as these elements are also identified in the chemical structure of the respective drug.

CONCLUSION

In conclusion, weight loss and potentiodynamic polarization (PDP) results demonstrate that the Lopinavir–Ritonavir co-formulation is an effective corrosion inhibitor for mild steel, achieving inhibition efficiencies of up to 95.70% and 93.0% at the optimum concentration. Adsorption of LPV–RTV follows the Langmuir isotherm and occurs spontaneously, predominantly via physical adsorption. The positive shift in corrosion potential (E_{corr}) to +105 mV/SCE indicates predominant suppression of the anodic metal dissolution reaction. SEM–EDX analysis further confirms adsorption of the drug molecules on the mild steel surface, supporting the formation of a protective film.

REFERENCES

1. Koch, G. H., Thompson, N. G., Moghissi, O., Payer, J. H., & Varney, B. (2016). International measures of prevention, application, and economics of corrosion technologies (IMPACT) study. NACE International. Report No. OAPUS310GKOCH.
2. Fontana, M. G. (2005). Corrosion engineering (3rd ed.). Tata McGraw-Hill.
3. Pathak, R. K., & Mishra, P. (2016). Drugs as corrosion inhibitors: A review. International Journal of Science and Research, 5(4). https://doi.org/10.21275/v5i4.NOV162623
4. Verma, C., Olasunkanmi, L. O., Obot, I. B., Ebenso, E. E., & Quraishi, M. A. (2016). 2,4-Diamino-5-(phenylthio)-5H-chromeno[2,3-b]pyridine-3-carbonitriles as green and effective corrosion inhibitors: Gravimetric, electrochemical, surface morphology and theoretical studies. RSC Advances, 6, 53933–53948. https://doi.org/10.1016/j.molliq.2018.06.110

5. Risto, S. C., & Karen, L. G. (2003). Lopinavir/ritonavir: A review of its use in the management of HIV infection. Drugs, 63(8), 769–802. https://doi.org/10.2165/00003495-200363080-00004
6. ASTM International. (1999). ASTM G1: Standard practice for preparing, cleaning, and evaluating corrosion test specimens. ASTM International.
7. Ansel, H. C., & Stockton, S. J. (2017). Pharmaceutical calculations (15th ed.). Wolters Kluwer.
8. ASTM International. (2012). ASTM G31-12a: Standard practice for laboratory immersion corrosion testing of metals. ASTM International.
9. Onen, A. I., Bulama, S., Kolo, A. M., Ebenso, E. E., & Apagu, D. A. (2019). Gravimetric and electrochemical studies of Balanites aegyptiaca DEL. ethanolic leaves extract as corrosion inhibitor for duplex stainless steel in 1.0 M HCl solution. FUW Trends in Science and Technology Journal, 4(3), 773–777.
10. ASTM International. (2003). ASTM G59-97: Standard test method for conducting potentiodynamic polarization resistance measurements. ASTM International.
11. Shwetha, K. M., Praveen, B. M., & Devendra, B. K. (2024). A review on corrosion inhibitors types, mechanism, electrochemical analysis, corrosion rate and inhibition efficiency of corrosion inhibitors on mild steel in acidic environment. Results in Surfaces and Interfaces, 16, 1–19. https://doi.org/10.1016/j.rsurfi.2024.100258
12. Karthik, G., & Sundaravadivelu, M. (2015). Studies on the inhibition of mild steel corrosion in hydrochloric acid solution by atenolol drug. Egyptian Journal of Petroleum, 25, 183–191. https://doi.org/10.1016/j.ejpe.2015.04.003
13. Abdallah, M., Soliman, K. A., Alfakeer, M., Hawsawi, H., Al-Bonayan, A. M., Al-Juaid, S. S., Abd El Wanees, S., & Motawea, M. S. (2023). Expired antifungal drugs as effective corrosion inhibitors for carbon steel in 1 M HCl solution: Practical and theoretical approaches. ACS Omega, 8, 34516–34533. https://doi.org/10.1021/acsomega.3c03257
14. Al-Mhyawi, M., Soliman, S., & Arafa, E. I. (2022). Evaluation of expired Augmentin drugs as corrosion inhibitor for carbon steel alloy in 1.0 N HCl acidic environment using analytical techniques. Egyptian Journal of Chemistry, 65(4), 735–745. https://doi.org/10.21608/ejchem.2021.95853.4495
15. Ikeuba, I. A., Aondoakan, L., Azagare, W., Njoku, C. N., Usibe, B. E., & Eche, O. (2025). Computational and experimental evaluation of the corrosion inhibition of magnesium in the presence of acids/esters in saline solutions. Current Research in Green and Sustainable Chemistry, 10, 1–12. https://doi.org/10.1016/j.crgsc.2025.100452
16. Obot, I. B., & Obi-Egbedi, N. O. (2010). Adsorption properties and inhibition of mild steel corrosion in sulphuric acid solution by ketoconazole: Experimental and theoretical investigation. Corrosion Science, 52(1), 198–204. https://doi.org/10.1016/j.corsci.2009.09.002
17. Toghan, A., Gadow, H. S., Fawzy, A., Hanan, A., & Salah, H. (2023). Adsorption mechanism, kinetics, thermodynamics, and anticorrosion performance of a new thiophene derivative for C-steel in 1.0 M HCl: Experimental and computational approaches. Metals, 13, 1–22. https://doi.org/10.3390/met13091565
18. Quraishi, M. A., Ansari, K. R., Yadav, D. K., & Ebenso, E. E. (2012). Corrosion inhibition and adsorption studies of some barbiturates on mild steel/acid interface. International Journal of Electrochemical Science, 7, 12301–12315. https://doi.org/10.1016/S1452-3981(23)16546-1
19. Reddy, M. J., Verma, C., Ebenso, E. E., Singh, K. K., & Quraishi, M. A. (2014). Electrochemical and thermodynamic investigation of nitrofurantoin as effective corrosion inhibitor for mild steel in 1 M hydrochloric acid solution. International Journal of Electrochemical Science, 9, 4884–4899.
20. Nsude, O. P., & Orie, K. J. (2022). Thermodynamic and adsorption analysis of corrosion inhibition of mild steel in 0.5 M HCl medium via ethanol extracts of Phyllanthus mellerianus. American Journal of Applied Chemistry, 10(3), 67–75. https://doi.org/10.11648/j.ajac.20221003.12
21. Alamry, K. A., Khan, A., Aslam, J., Hussein, M. A., & Aslam, R. (2023). Corrosion inhibition of mild steel in hydrochloric acid solution by the expired ampicillin drug. Scientific Reports, 13, 6724. https://doi.org/10.1038/s41598-023-33519-y
22. Ansari, K. R., Quraishi, M. A., Prashant, & Ebenso, E. E. (2013). Electrochemical and thermodynamic investigation of diclofenac sodium drug as a potential corrosion inhibitor for mild steel in hydrochloric acid. International Journal of Electrochemical Science, 8, 12860–12873. https://doi.org/10.1016/S1452-3981(23)13312-8

23. Ebenso, E. E., & Obot, I. B. (2010). Inhibitive properties, thermodynamic characterization, and quantum chemical studies of secnidazole on mild steel corrosion in acidic medium. International Journal of Electrochemical Science, 5, 2012–2035. https://doi.org/10.1016/S1452-3981(23)15402-2
24. Kuang, F., Zhang, J., Zou, C., Shi, T., Wang, Y., Zhang, S., & Xu, H. (2010). Electrochemical methods for corrosion monitoring: A survey of recent patents. Recent Patents on Corrosion Science, 2, 34–39. https://doi.org/10.2174/1877610801002010034
25. Aldana-González, J., Espinoza-Vázquez, A., Romero-Romo, A., Uruchurtu-Chavarín, A., & Palomar-Pardavé, M. (2019). Electrochemical evaluation of cephalothin as corrosion inhibitor for API 5L X52 steel immersed in an acid medium. Arabian Journal of Chemistry, 12, 3244–3253. https://doi.org/10.1016/j.arabjc.2015.08.033
26. Obot, I. B., Ebenso, E. E., & Kabanda, M. M. (2013). Metronidazole as an environmentally safe corrosion inhibitor for mild steel in 0.5 M HCl: Experimental and theoretical investigation. Journal of Environmental Chemical Engineering, 1, 431–439. https://doi.org/10.1016/j.jece.2013.06.007
27. Edison, T. J. I., & Sethuraman, M. G. (2013). Electrochemical investigation on adsorption of fluconazole at mild steel/HCl acid interface as corrosion inhibitor. ISRN Electrochemistry, 1–8. https://doi.org/10.1155/2013/256086
28. Quraishi, M. A., Yadav, D. K., & Ahamad, I. (2015). Corrosion inhibition of mild steel in 1 M HCl by some newly synthesized pyrimidine derivatives: Electrochemical and quantum chemical studies. Journal of Industrial and Engineering Chemistry, 21, 1176–1185.
29. Singh, P., Ebenso, E. E., Olasunkanmi, L. O., Obot, I. B., & Quraishi, M. A. (2016). Electrochemical, theoretical, and surface morphological studies of corrosion inhibition effect of green naphthyridine derivatives on mild steel in hydrochloric acid. Journal of Physical Chemistry C, 120, 3408–3419. https://doi.org/10.1021/acs.jpcc.5b11901
30. Abdel-Hameed, R. S., Qureshi, M. T., Abdallah, M., Aljuhani, E., Alzharani, A. A., Alfarsi, A., Bakry, A. M., Huwaimel, B., & Farghaly, O. (2022). Recycling of expired lactulose drugs as eco-friendly corrosion inhibitor for steel alloys in acidic environment: Gravimetrical and electrochemical studies. International Journal of Electrochemical Science, 17, 1–16. https://doi.org/10.20964/2022.12.92
31. Rugmini, P., Ammal, M. P., & Joseph, A. (2018). Physicochemical studies on the inhibitive properties of a 1,2,4-triazole Schiff's base on mild steel corrosion in hydrochloric acid. Egyptian Journal of Petroleum, 27, 307–317. https://doi.org/10.1016/j.ejpe.2017.05.002
32. Rosliza, R., & Izman, S. (2011). SEM-EDX characterization of natural products on corrosion inhibition of Al-Mg-Si alloy. Journal of Physicochemical Problems of Materials Protection, 47, 395–401. https://doi.org/10.1134/S2070205111030129
33. Peme, T., Olasunkanmi, L. O., Bahadur, I., Adekunle, A. S., Kabanda, M. M., & Ebenso, E. E. (2015). Adsorption and corrosion inhibition studies of some selected dyes as corrosion inhibitors for mild steel in acidic medium. Molecules, 20, 16004–16029. https://doi.org/10.3390/molecules200916004